

## **MATHEMATICAL MODEL FOR MICRO-IRRIGATION DESING FOR CENTER PIVOT CORNERS**

**Guirguis, A. E.<sup>1</sup>; A.A. El-Shafei<sup>2</sup> and K. A. Allam<sup>1</sup>**

**<sup>1</sup>Agric. Engineering Res. Inst. Agric. Res. Center, Dokki, Giza, Egypt.**

**<sup>2</sup>Agric. Engineering dept., Fac. of Agric., Alexandria University.**

### **ABSTRACT**

A mathematical model was developed to analyzing hydraulic characteristics in a micro-irrigation system design micro-irrigation system for center pivot corners. Different shape division (square, rectangular and approximately triangular shape) for center pivot corner, pipe diameters and lengths of lateral and telescopic manifold pipe with uniform slopes were studied. The model divided the center pivot corner into subunits micro-irrigation system (parts) and estimated lateral and emitter discharges and pressure head distribution along a lateral and manifold starting from the downstream as well as uniformity calculation. The friction head loss between successive emitters, laterals and manifold were also estimated using the Darcy-Weisbach formula. The model for designing manifold was run successfully for supplying water to one or two-side laterals. Field studies were undertaken to test the validity of the mathematical model for ( $E_u$ ), ( $U_c$ ), ( $Q_{VAR}$ ) and ( $H_{VAR}$ ). Emission flow and pressure distributions were measured and compared quite well with those predicted from the model. The results indicated that, for approximately triangular shape part 1 for center pivot radius 450 m, outside lateral diameter 16 mm, lateral spacing 1.0 m and emitter spacing 0.5 m, average emitter discharge per lateral for 76 lateral were ranged from 3.618 to 3.766 l/h. Lateral dynamic head increased from 0.81 to 1.26 bar for 76 lateral, ( $U_c$ ), increased by 7.42% and ( $U_c$ ) increased with decreasing lateral friction losses, Inlet lateral discharge for 76 laterals were ranged from 7.1 to 240.6 l/h for minimum (2 m) and maximum (63 m) lateral lengths, respectively. The model has been verified under different three center pivot radiuses (270, 359 and 450 m), which have same lateral diameter (16 mm), emitter spacing 1.0 m, lateral spacing 2.5 m and same in-line emitter discharge equation  $q=4.02H^{0.5}$  as an example for grape cultivation. Also, three different outside lateral diameters 16, 18 and 20 mm which, has same emitter spacing 0.5 m, lateral spacing 1.0 m and the same emitter type with constant center pivot radius (450 m) were verified for strawberry cultivation. In comparison between model output results of center pivot corner with  $R=450$  m for lateral diameters 18 and 20 mm, it is clear that the number of parts dose not changed (13 parts) and total manifold discharge was equal to 313.46 ( $m^3/h$ ) for both lateral diameters. While, number of parts was (19 parts).for lateral diameters 16 mm.  $Q_{VAR}$  at lateral diameter 18 and 20 mm were ranged from 0.7 to 6.51% and 0.47 to 4.35% respectively. Also,  $H_{VAR}$  were ranged from 1.14 to 12.59% and 0.94 to 8.52% respectively. However, lateral diameter 20 mm was more effective in improving ( $Q_{VAR}$ ) and ( $H_{VAR}$ ). In case of  $R=450$  m for lateral diameters 16 mm, manifold diameters 50, 63, 75 and 90 mm versus lengths were 641, 185, 97 and 92 m respectively, while, manifold length were 505, 182, 91 and 158 m for lateral diameters 18 mm.

**Keywords:** Micro-irrigation, design, model, subunit, hydraulic.

### **INTRODUCTION**

Centre-pivot irrigation system one of the most popular systems for irrigation general field crops especially in arid and semi-arid regions. The center pivot cannot irrigate the whole square area, where it irrigates circular

area, and there are four corners area can't be irrigated by this system. The corners area that not irrigate represents the percentage of, 21.5% of the total square area. To maximize the usability of horizontal expanded areas that irrigate by center pivot irrigation system, the farmers irrigate the corners by drip irrigation system. There is a few literature and information concerning the design of center pivot corners with drip irrigation system. That led to reduce efficiency of drip irrigation system in these corners, due to low executive experiences. They dose not putting in their concern the standard design items such as discharge variation ( $Q_{VAR}$ ), pressure head variation ( $H_{VAR}$ ), emission uniformity ( $E_U$ ), uniformity coefficient ( $U_C$ ). The purpose of this study is to putting some designing attempts for corners drip irrigation system network to increase drip irrigation efficiency especially ( $Q_{VAR}$ ), not exceeded than 10% and ( $H_{VAR}$ ) not exceeded than 20%, according to ASAE standards (1996).

Guirguis et al (2009) developed a deterministic model for designing subunit drip irrigation system for uniform shape. Different pipe diameters and lengths of lateral and telescopic manifold pipe with uniform slopes were studied. The model estimated lateral and emitter discharges and pressure head distribution along a lateral and manifold starting from the downstream as well as uniformity calculation. The friction head loss between successive emitters, laterals and manifold were estimated using the Darcy-Weisbach formula. The change of the velocity head, the changes of momentum along the lateral and manifold and the loss due to emitter connection were also considered. The model for designing manifold was run successfully for supplying water to one-side and two-side laterals.

ASAE (1993c and 2002a), Smith (2003) and Sharaf (2004b) indicated that lateral length and slope have greater effect on subunit uniformity than manifold length and slope. The water temperature has no influence on subunit water uniformity.

Zella and Kettab (2002) micro-irrigation is used in the arid and semi-arid countries. In their study a network is composed of laterals with identical emitters that have a small discharge to low pressure. The network must satisfy a good uniformity of water distribution by emitters to the irrigated plants. Thus, the hydraulic phenomenon study of the lateral is primordial for the adequate and economic network design. For the lateral, other than changes in elevation, variations of the pressure are due to the energy loss of friction along the lateral that provokes disorder to the uniformity of the water distribution. They also contribute to the hydraulic analysis of the lateral micro-irrigation by using the numerical methods: They found that the models of calculation used have the advantage to be simple, fast, precise, and allow their extension to large micro-irrigation network. The discharge of emitter is also influenced by the temperature (air and water) but it seems that the effect is mostly negligible when the flow is turbulent, except perhaps in desert conditions. Micro-irrigation design should determine the dimensions of plot and network, so that the system will be as economically efficient as possible. Each case requires its own analysis and design nevertheless it's possible to give a few indications about the size of irrigation plots and their shape.

Zella et-al.(2006) using the back step procedure to design a micro-irrigation system based on control volume method Their study included proposed numerical method was simple and consists of delimiting an elementary volume of the lateral equipped with an emitter, called « control volume » on which the conservation equations of the fluid hydrodynamic's are applied. Also they developed a simple microcomputer program and used for the calculation and the convergence estimated, average water requirement of plants to choose the sum of the average emitter discharge as the total average flow rate of the network.

Antonina and Scicolone (1998). Al-Misned et al. (2000) reported that, the estimation of energy losses due to emitter's connection in micro-irrigation laterals is very important. Since these losses have a direct effect on micro-irrigation system design, the study of these losses will lead to the improvement of system efficiency which will eventually result in conservation of water and energy.

The objectives of this work are: 1- developing a mathematical model for dividing and designing subunit micro-irrigation system for center pivot corner including laterals and manifolds hydraulic design to estimate both of ( $Q_{VAR}$ ), ( $H_{VAR}$ ), ( $E_u$ ) and ( $U_c$ ). 2- check model validation results compared with experimental field data. 3-testing model verification in designing center pivot corners with different radiuses that available commercially.

### **Theoretical Approach And Model Procedding**

## Lateral line hydraulics design

The proposed computation model for center pivot corner area was based upon equations of conservation of mass and energy. In modeling, it was assumed that emitters on micro-irrigation lines were installed at an equal spacing;  $s$ . The first upstream emitter was at a different spacing:  $s_1$ , from the manifold. The equation describes emitter discharge was expressed as

where,  $q_n$  is the discharge of emitter  $n$ ,  $c$  is an emitter coefficient that accounts for area and discharge effect,  $H_n$  = the pressure head acting on the emitter  $n$ , and  $y$  = the emitter exponent constant, which depends on the state of flow and ranges from zero and 1.0.

As the lateral line has  $n$  emitters and the lateral end is closed, the discharge down stream from the emitter  $n$  should be zero, therefore,  $Q_n = 0.0$ . The lateral discharge upstream from emitter  $n$  should equal the emitter discharge;  $Q_{n-1} = q_n$ .

In modeling, the conservation of energy equation through lateral line between emitters  $n$  and  $n-1$  was used as expressed by Hathoot et al. (1993). The equation was based on the Darcy-Weisbach friction head loss and the momentum effect resulting from decreasing the discharge through lateral from  $Q_{n-1}$  to  $Q_n$ . The pressure head acting on emitter  $n-1$  was given by:

$$H_{n-1} = H_n - \frac{3}{2gA^2} \left[ (Q_n + q_n)^2 - Q_n^2 \right] + \frac{8f_{n-1}}{\pi^2 g D^5} \frac{s(Q_n + q_n)^2}{\pm (Z_n - Z_{n-1})} \quad .(2)$$

Where,  $A$  = the cross-sectional area of lateral,  $g$  = the acceleration due

to gravity,  $D$  = the lateral diameter, the positive sign corresponds to laterals sloping upwards and the negative sign is for downward slope,  $z_1$  and  $z_o$  = elevation of emitters, respectively, and  $f_{n-1}$  = the coefficient of friction in the lateral reach between emitters  $n-1$  and  $n$ , which is depending on Reynolds number;  $R$ . In case of  $R \leq 2000$  (Laminar),  $f = 64/R$ ,  $3000 \leq R \leq 10^5$  (Turbulent),  $f = 0.316 R^{-0.25}$  and  $10^5 \leq R \leq 10^7$  (Fully turbulent flow),  $f = 0.13 R^{-0.172}$

Mathematical model estimates the pressure head distribution along a lateral starting from the downstream reach of the manifold line. The pressure head at the manifold;  $H_0$  was calculated from:

## Uniformity calculation

**Emission uniformity,  $E_u$**  is defined as the relationship between the minimum (or maximum) emitter discharge and the average emitter discharge within a lateral.

**Christiansen uniformity coefficient,  $U_c$**  is a good measure of the uniformity (Keller and Karmelli, 1974), which is given by:

$$U_C = 1 - \left[ \frac{1}{n \cdot q_{ave}} \right] \sum_{i=1}^n |q_i - q_{ave}| \quad \dots \quad (3)$$

where,  $q_{ave}$  = the average discharge of  $n$  emitters.

### Lateral discharge and operating pressure head variations

The ASAE standards (1996) stated that to perform acceptable uniformity in micro-irrigation field, the maximum discharge and pressure head variations should not exceed than 10% and 20%, respectively. The calculation of the maximum discharge variation and pressure head variation between emitters along the lateral design were estimated for each lateral along the manifold length.

## Prediction of lateral length:

Micro-irrigation lateral design for center pivot corner area can be classified into three types of design problems. 1-lateral length is unknown but pipe size is constrained, 2-pipe size is unknown but lateral length is constrained and 3-neither pipe size nor lateral length are constrained. In this study case one was considered. The objective is normally to determine the maximum lateral length, which can be utilized for pipe size while maintaining a specific uniformity coefficient of about 95% equal an emitter flow variation of 10%.

## **Manifold line hydraulics design**

The first assumption in manifold design is the lateral discharge;  $Q_L = Q_0$ , The discharge of last downstream segment manifold is equal to last lateral discharge, then  $Q_M = Q_L$ . The discharge of second downstream segment manifold ( $Q_{M-1}$ ) is equal to last lateral discharge ( $Q_L$ ) plus second downstream lateral discharge ( $Q_{L-1}$ ), then  $Q_{M-1} = Q_L + Q_{L-1}$ . The change between ( $Q_L$ ) and ( $Q_{L-1}$ ) was due to the segment manifold friction losses. The followed segment manifold discharge was equal to the cumulative laterals discharge and could be expressed as the following equation:

$$Q_{M-1} = Q_M + Q_{L-1} \quad \dots \quad (4)$$

According to total segment manifold discharge, the modeling select first manifold pipe type and the inside diameter which, proportional to maximum

discharge of manifold design. In case of  $Q_M < 8400.0$  outside manifold diameter equal to 50 mm,  $8400.0 \geq Q_M < 14100.0$  outside manifold diameter equal to 63 mm,  $14100.0 \geq Q_M < 20000.0$  outside manifold diameter equal to 75 mm and  $Q_M > 20000.0$  outside manifold diameter equal to 90 mm.

The coefficient of friction due to different segment manifold discharge was calculated by using the above equations and the total head loss was also estimated to find the total segment manifold operating head, which was used as total operating head for second lateral. Ismail (1993) reported that, to provide first estimation for the change in the lateral discharge, the discharge of the lateral could be calculated as a function of the inlet operating head as follows:

Where:  $Q_L$  = discharge entering the lateral, ( $l/h$ ),  $H$ = operational head at the lateral inlet (m),  $A$ = constant representing the lateral diameter and dimensions and  $X$ = constant representing the flow regime of the lateral.

The modeling calculated the coefficients  $A$  and  $X$  by finding the two lateral flow rates and the corresponding inlet lateral operating pressure heads. The calculations of the coefficients  $A$  and  $X$  were estimated for every two successive lateral discharge along the manifold length. Also the cumulative friction loss was estimated and the total operating head was also determined by modeling for both of each lateral and each segment manifold. By the same way the total operating head was calculated for total manifold line to estimate the subunit water horsepower needed.

### Prediction of telescopic manifold diameters and lengths:

The model selected and asked first if manifold supply water to one or two side lateral, then calculated the total segment manifold discharge. The selected diameter was chosen according to maximum manifold discharge. Also the cumulative segment manifold length was determined by the modeling. The modeling changes the diameter according to total manifold discharge.

#### **Prediction of new average emitter discharge in previous lateral:**

New emitter discharge in previous lateral was determined by using the following equation:

Where:  $qq_n$ : emitter discharge closed to lateral end ( $l/h$ ),  $COL$ : calculated new lateral discharge ( $l/h$ ),  $Q_{MAX}$ : theoretical maximum lateral discharge ( $l/h$ ),  $N$ : number of emitter in or on lateral and  $Q_{END}$ : the average emitter discharge in or on lateral ( $L-1$ ) ( $l/h$ ).

### **Subunit discharge and operating pressure head variations**

The calculations of discharge and pressure head variations between emitters along the lateral design were estimated for each lateral along the manifold length. Then, the subunit  $Q_{VAR}$  and  $H_{VAR}$  were determined for all laterals between maximum and minimum emitter discharge and operating head.

### **Designing area of center pivot corner:**

- 1- Model designs whole area of center pivot corner as one part; where

manifold line was parallel to horizontal Cartesian and lateral lines were perpendicular on the manifold in one side direction. Then, the model provides information about the values of discharge variation;  $Q_{VAR}$  and pressure head variation;  $H_{VAR}$ . Comparison between the estimated values of  $Q_{VAR}$  and  $H_{VAR}$  and the values of allowable  $Q_{VAR}$  and  $H_{VAR}$  (10 and 20%), were done by the model. If the estimated values exceeded than the allowable, the model rerun again after dividing whole area into three parts (square and two approximately triangular shapes) as shown in Fig. (1A).

The dimension of square shape was estimated by model using the following equation

where:  $R$  is center pivot radius (m), and the dimension of approximately triangular shape were  $X$  and  $R - X$ .

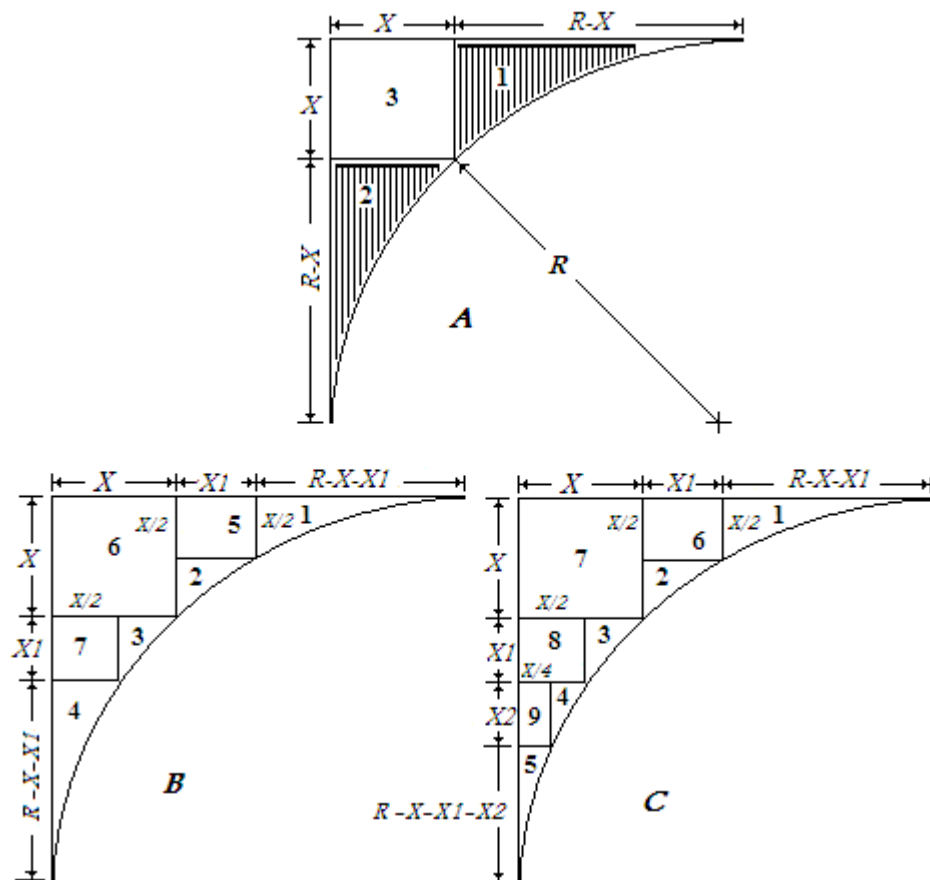


**Fig. (1) Modeling design steps for dividing whole area of center pivot corner.**

2- For square shape, the model run first the whole area of square shape as one part and manifold line was parallel to horizontal Cartesian with length

(X). Lateral lines were perpendicular on the manifold in one side direction with length of (X). If  $Q_{VAR}$  and  $H_{VAR}$  greater than the allowable values, (10 and 20%), the model divided the lateral line into two lengths (each length is equal to  $X/2$ ) and the length of manifold line (X) in two lateral side directions as shown in Fig. (2A).

If  $Q_{VAR}$  and  $H_{VAR}$  greater than the allowable values, the model divided the manifold line into two lengths (each length is equal to  $X/2$ ) and the length of lateral line ( $X/2$ ) as shown in Fig. (2B). If  $Q_{VAR}$  and  $H_{VAR}$  still greater than the allowable values, The model continued in dividing area of square shape into small parts, as shown in Fig (2C) and Fig (2D) until  $Q_{VAR}$  and  $H_{VAR}$  reached to the allowable values (10 and 20%).

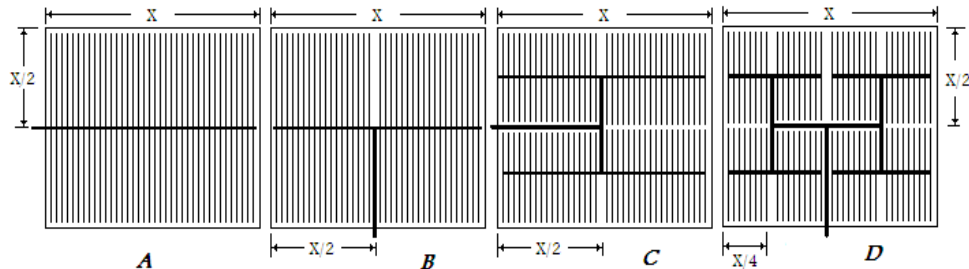


Fig (2) Model design steps for dividing whole area of square shape for center pivot corner.

3- For approximately triangular shape, the model run the whole area as one part as shown in Fig. (2A). If  $Q_{VAR}$  and  $H_{VAR}$  greater than the allowable values (10 and 20%), the model divided the approximately triangular shape at horizontal and vertical directions into three parts (rectangular and two approximately triangular shapes) as shown in Fig.(1B).

- a- At horizontal direction, there is rectangular shape (part 5) and two approximately triangular shapes (parts 1 and 2).
  - b- At vertical direction, there is rectangular shape (part 7) and two approximately triangular shapes (parts 3 and 4).

4-The rectangular shape has a dimension of  $(X/2)$  and  $(X_1)$ .  $X_1$  was calculated from equation (8).

Calculations similar to that performed in step 2 were repeated until reached to  $Q_{VAR}$  and  $H_{VAR}$  less than the allowable values.

The dimensions of approximately triangular shape for part 1 and part 4 were ( $X/2$  and  $R-X-X_1$ ), while for part 2 and 3 were ( $X_1$  and  $X/2$ ).

5 For approximately triangular shape, the model compared the estimated values of  $Q_{VAR}$  and  $H_{VAR}$  for each part with the values of allowable  $Q_{VAR}$  and  $H_{VAR}$ . If the estimated values were exceeded than the allowable values, the model divided the approximately triangular shape into rectangular and two approximately triangular shapes (part 9, 4 and 5) as shown in Fig (1C).

The dimension of approximately triangular shape as in part 4 as shown

in Fig (1B), the length of (R-X-X<sub>1</sub>) was divided to (X<sub>2</sub>) and (R-X- X<sub>1</sub>- X<sub>2</sub>) as shown in Fig.(1C). X<sub>2</sub> was determined from the following equation:

$$X_2 = R - (X + X_1) - \sqrt{R^2 - (R - (X/2)/2)^2} \quad \dots \dots \dots \quad (9)$$

6- It is not necessary that the model is dividing the approximately triangular shape into the same number of parts in horizontal and vertical directions. According to the values of  $Q_{VAR}$  and  $H_{VAR}$  for approximately triangular shape, numbers of parts in vertical direction were varied than in horizontal direction. This because of in vertical direction, manifold length was shorter and lateral length was longer than in horizontal direction. Also the values of  $Q_{VAR}$  and  $H_{VAR}$  were depended on number of emitters on lateral length and emitter spacing.

7- The general equation for estimating any length for square or rectangular shapes at center pivot corner  $X_i$  was calculated from the following equation:

where: the values of  $Y_i$  and  $Z_i$  were calculated using model by the following equation

$$\begin{aligned} \text{For } i = 1: \quad & Y_i = X \quad \text{and} \quad Z_i = X \\ \text{For } i > 1: \quad & Y_i = Y_{i-1} + X_{i-1} \quad \text{and} \quad Z_i = X_{i-1}/2 \end{aligned} \quad \dots\dots\dots (11)$$

Notes that: a- In case of whole area of center pivot corner, the model run as one part, there is no  $X$  and  $X_i$ 's values. b- In case of dividing the whole area of center pivot corner by model into three parts (square and two approximately triangular shapes), there is no values of  $X_i$ 's while,  $X$  value appear as shown in Fig. (1A). c- In case of dividing the whole area of center pivot corner by model to more than three parts, the values of  $X_i$ 's were determined by model from general equation (equation 10).

8- In case of any part of approximately triangular shape, there is died area that, dose not contain lateral and manifold lines. The died length in the horizontal Cartesian was determined using model from the following equation:

$$DL_j = \sqrt{R^2 - \left[ \sqrt{R^2 - YY_j^2} - LL_{\min} \right]^2} - YY_j \quad \dots \dots \dots \quad (12)$$

Where:  $DL_j$  is the died length of any approximately triangular shape that dose not contain lateral and manifold lines,  $YY_j$  is the horizontal distance started from corner of center pivot to another corner of approximately triangular shape that has number ( $J$ ), and  $J$  is the number of approximately triangular shape started from the horizontal corner of center pivot.

9- Lateral length next to died area and lateral length at any point along manifold for center pivot corner were calculated by model using the following equations:

$$LL_{jl} = \sqrt{R^2 - YY_j^2} - \sqrt{R^2 - (YY_j + DL_j + SM \cdot (N_l - 1.0))^2} \quad \dots \quad (13)$$

10- After modeling selected the desired area (approximately triangular

shape or square shape or rectangular shape), lateral line hydraulics design was done by model for estimating the following values of minimum and maximum lateral length, number of emitters per lateral, number of laterals per part (subunit area), each emitter discharge and operating head, average emitter discharge per part, friction loss in segment lateral, lateral dynamic head, lateral emission uniformity ( $E_u$ ), uniformity coefficient ( $U_c$ ), discharge variation ( $Q_{VAR}$ ) and pressure head variation ( $H_{VAR}$ ) between emitters along any lateral.

11- For manifold line hydraulics design, the telescopic manifold diameter was chosen carefully by model according to maximum manifold discharge passes through it. Also the cumulative segment manifold length and discharge were estimated, friction loss in segment manifold and manifold dynamic head.

12- The overall values of ( $E_u$ ), ( $U_c$ ), ( $Q_{VAR}$ ) and ( $H_{VAR}$ ) were also estimated by model for each part individually, of micro-irrigation center pivot corner network.

## **MATERIAL AND METHODS**

In order to validate the model of designing irrigation subunit center pivot corner network, an area of center pivot corner for Grape were tested for center pivot radius 450 m with 16 mm lateral diameter. Field experiment was conducted during summer season 2008 at Company of Agricultural Alexandria, West Nubaria, Behera, Egypt. The subunit micro-irrigation network were implemented and equipped with a control head consisting of electrical centrifugal pump, non-return valve, pressure regulator, sand and screen filters, control valves, pressure gauges and flow meter. For comparison between predicted data from model and field experiment data, the average distribution of emitters' discharge along laterals for far approximately triangular shape of center pivot corner were measured. The inlet and tail end of each lateral line along manifold were plugged with pressure gauge and recorded for three times. Water temperature was also measured to account viscosity changes. The input data for modeling subunit micro-irrigation system was consisting of polyethylene lateral length started from minimum lateral length (2.0 m) to maximum lateral length, emitter spacing = 1.0 m, lateral spacing = 2.5 m (No. of laterals along manifold depending on manifold length). Number of emitters along each lateral for any approximate triangular shape was varied according to predicted lateral length. In-line emitter type equation;  $q = 4.02 H^{0.50}$ , lateral and manifold slopes = 0%, assumed operating emitter pressure head equal 1 bar, and intended coefficient of uniformity;  $U_c = 0.95$ .

The model was predicted lateral length, diameter of telescopic manifold pipes, head and discharge of each emitter along each lateral, inlet lateral head and discharge along manifold, friction losses through lateral and manifold segment, and statistical items such as variation of emitter discharge ( $Q_{VAR}$ ) and head ( $H_{VAR}$ ), standard deviation, coefficient of variation, emission uniformity ( $E_u$ ), uniformity coefficient ( $U_c$ ) for each lateral and as overall subunit irrigation network.

The flow chart diagram of the computer program is shown in Fig. (3). Essential parameters such as center pivot radius, lateral diameter, land slope, emitters spacing, the average pressure head, the emitter constant  $c$  and the exponent  $y$ , should be known in advance.

## RESULTS AND DISCUSSIONS

### Modeling results validation

Model validation was done between the theoretical model values and the experimental observed values for Grape center pivot corner area ( $R=450$  m and  $D=16$  mm lateral diameter). For approximately triangular shape part 1, the computation using model provided the values of average values of emitter discharge per lateral for 76 lateral along manifold, discharge and pressure head of inlet lateral along manifold, average value for both of lateral discharge variation ( $Q_{VAR}$ ), pressure head variation ( $H_{VAR}$ ), average value for both of emission uniformity ( $E_U$ ) and uniformity coefficient ( $U_c$ ).

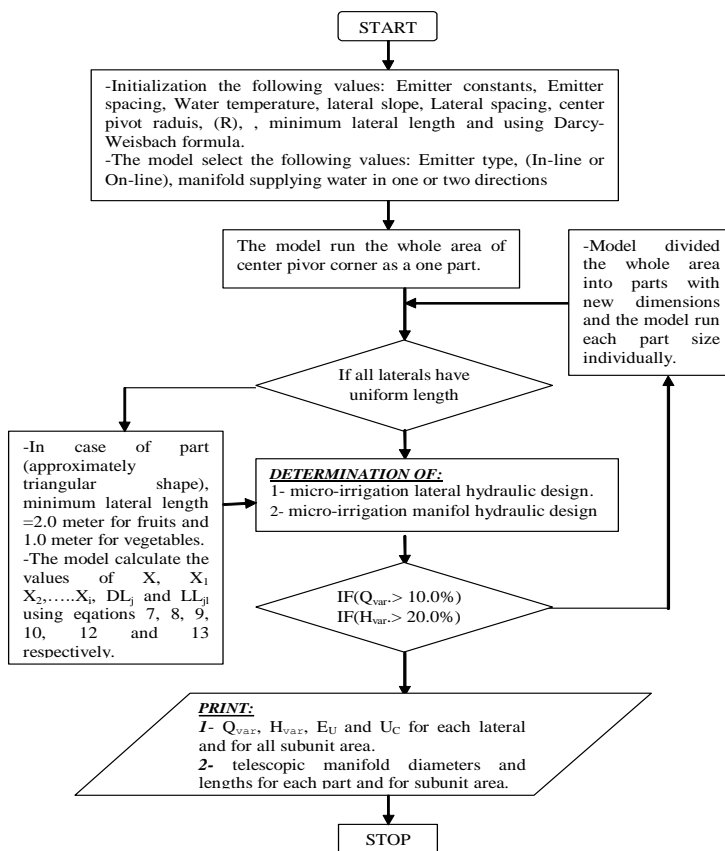


**Fig. (3) Center pivot corner micro-irrigation design flow-chart**

The average deviation percentage for average emitter discharges per lateral for 76 laterals along manifold, through part one as shown in Fig (1C), for approximately triangular shape center pivot corner was 1.18%. Statistical analyses showed that the determination of the correlation coefficient ( $R^2$ ) between predicted and measured values of average emitter discharges per lateral, for 76 laterals was 0.97. Results indicated that the model is capable of predicting any average emitter discharge ( $q_{AVE}$ ) per lateral for any approximately triangular shape with high accuracy.

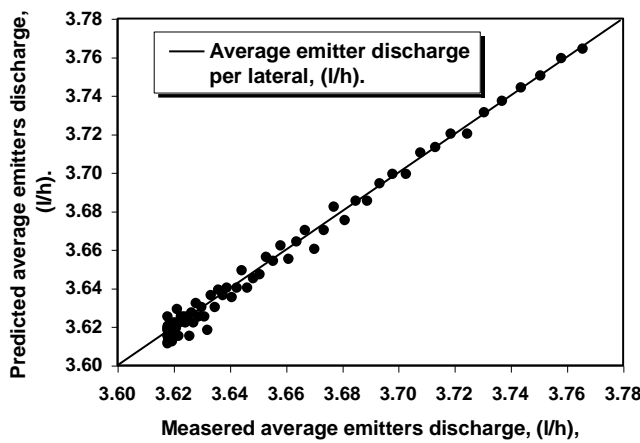


**Fig. (4) Measured and predicted average emitter discharge per lateral along manifold for approximately triangular shape part 1.**

Fig. (5A) and (5B) illustrate measured and predicted values of emitter discharge and operating head variations. The average deviation percentage of discharge and head variations per lateral for 76 laterals along manifold, for approximately triangular shape, part one as shown in Fig (1C), were equal to 1.93 and 2.61% with correlation coefficient ( $R^2$ ) 0.96 and 0.95, respectively. This means that the predicted values of discharge variation and head variation are closely agreement with the experimental observed values. These results were confirmed with Al-Amoud (1997) and Smith (2003).

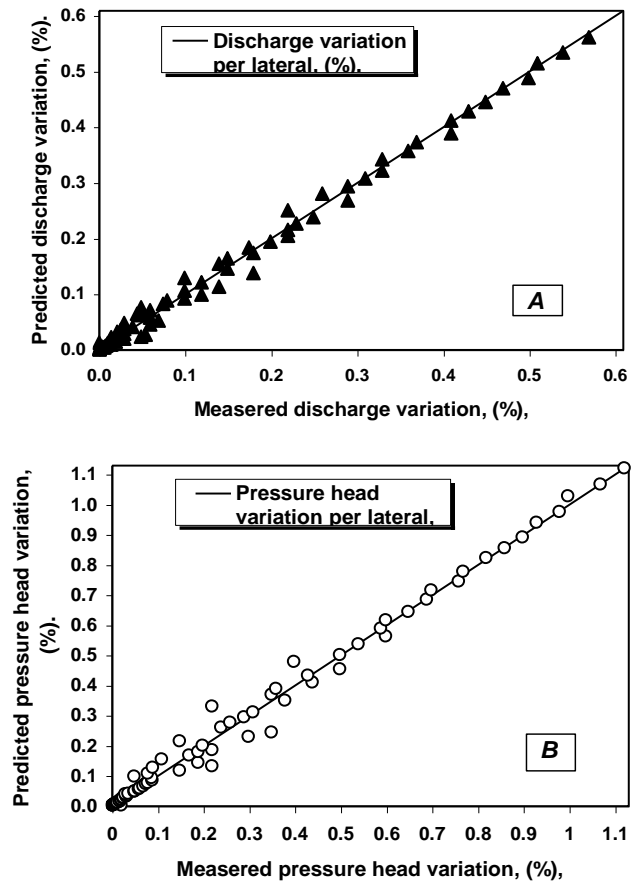


**Fig. (5) Measured and predicted emitter discharge variation ( $Q_{VAR}$ ) and pressure head variation ( $H_{VAR}$ ) per lateral along manifold for approximately triangular shape part 1.**

Fig (6A) and (6B) illustrate measured and predicted values of emission uniformity and uniformity coefficient per lateral for 76 laterals along manifold for approximately triangular shape, part one. It clear that the average deviation percentage for emission uniformity and uniformity coefficient per lateral for 76 laterals along manifold were equal to 2.16 and 2.22% with correlation coefficient ( $R^2$ ), 0.97 and 0.96, respectively. High values of correlation coefficient ( $R^2$ ) indicate that the predicted values are closely agreement with the experimental data. The result shows that, the model operates well and converges quickly toward fixed solution at the desired uniformity coefficient. The uniformity of emitter coefficient is superior to 94.92% in order to analyze such as large micro-irrigation system accurately, the task of calculating the pressure and discharges for each emitter becomes

enormous so it's important to choose this computation method. These results were confirmed with EL-Nesr (1999) and Zella et al. (2006).

Water uniformity ( $\approx 95\%$ ) guaranteed to satisfy water needs of plants when variations of pressure and emitter discharge were, respectively, less than 20 and 10%. Lateral pressure head increased from 0.81 to 1.26 bar for 76 lateral in part one as shown in Fig (1C), uniformity coefficient increased by 7.42%. Uniformity coefficient, ( $U_c$ ) increased with decreasing lateral friction losses. Lateral friction losses for the same above condition were ranged from  $3.4 \times 10^{-5}$  to 0.37 bar for minimum (2 m) and maximum lateral length (63.1 m) along manifold, respectively. These results were confirmed with Zella et al. (2002).

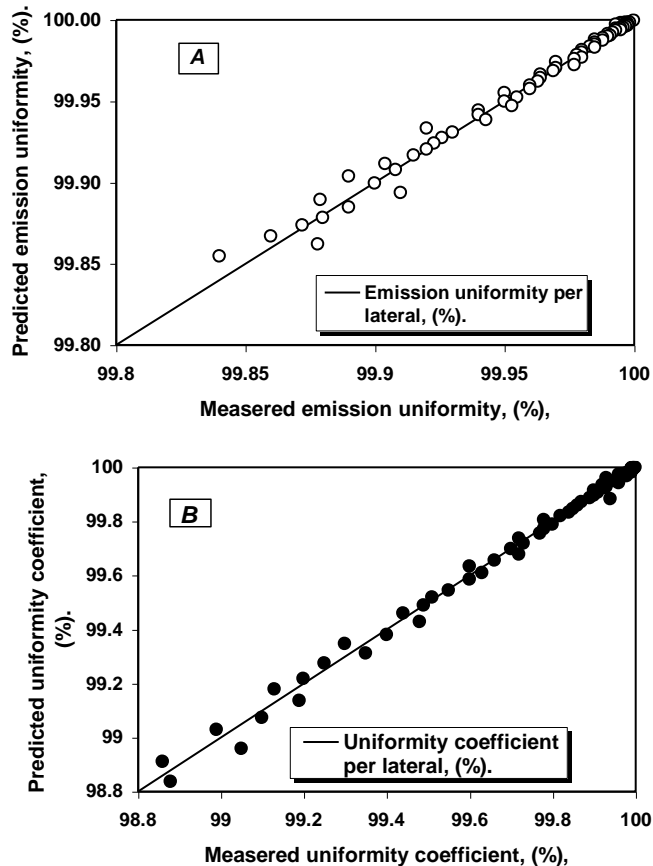


**Fig. (6) Measured and predicted emission uniformity ( $E_u$ ) and uniformity coefficient ( $U_c$ ) per lateral along manifold for approximately triangular shape part 1.**

The discharge passes through segment manifold in approximately triangular shape for grape center pivot corner area as in part one as shown in

Fig (1C), ( $R=450$  m, with 16 mm lateral diameter), were ranged from  $7.24 \times 10^{-3}$  to  $6.85$  ( $m^3/h$ ). Low value of segment manifold discharge ( $7.24 \times 10^{-3} m^3/h$ ) depending on number of emitters (2 emitters) for minimum lateral length next to dead area, while maximum segment manifold discharge ( $6.85 m^3/h$ ) depending on number of emitters (63 emitter) in maximum lateral length. These results were agreement with Zella et al. (2006).

The telescopic manifold lengths versus diameters were selected and chosen carefully by model for one or two sides lateral were predicted for subunit micro-irrigation network. For example part 1 for approximately triangular shape as shown in Fig (1C), ( $R=450$  m and  $D=16$  mm lateral diameter) the manifold lengths versus diameters was 50 meter for 90 mm. While, part 8 has dimensions of ( $X/2$ ) and ( $X/1$ ) as shown in Fig (1C), telescopic manifold lengths were 62.5 and 2.5 m for 50 and 63 mm manifold diameter, respectively. These result referred to and depending on maximum manifold discharge passing through different segment manifold, (number of laterals and emitters). This means that, the computer modeling successive accurately for selecting segment manifold length with diameter for desired  $U_C > 95\%$ . These results were agreement with EL-Nesr (1999) and Ismail et al. (2001).

Fig (7), presents the effect of lateral number along manifold versus measured inlet lateral discharge and pressure head along manifold for grape center pivot corner area, as shown in Fig (1C) for approximately triangular shape subunit at part 1, ( $R=450$  m, with 16 mm lateral diameter). It is noted, that inlet lateral discharges along manifold were ranged from 7.1 to 240.6 l/h for minimum and maximum lateral lengths 2 to 63.1 m, respectively. Inlet lateral head were slightly decreased which ranged from 0.915 bar (at lateral No.1) to 0.819 bar (at lateral No. 76) along manifold distance. The increase of segment manifold pressure head was due to high friction loss at upstream. High friction loss occurred at inlet segment manifold (closed to lateral No.1) due to large amount of water supplied. These results were confirmed with Amer and Gomaa (2003).

### **Model results verification**

In order to verify the model, six cases were executed to cover extremely field conditions under different center pivot corner areas for different lateral diameters, different emitter spacing and different lateral spacing. Three study cases represented three center pivot radii (270, 359 and 450 m), which have same lateral diameter (16 mm), emitter spacing (1 m), lateral spacing (2.5 m) and same in-line emitter discharge equation  $q=4.02H^{0.5}$  as an example for grape cultivation. While other study cases represented three different outside lateral diameters (16, 18 and 20 mm) which, has same emitter spacing (0.5 m), lateral spacing (1 m) and same in-line emitter equation  $q=4.02H^{0.5}$  with constant center pivot radius (450 m) for example strawberry cultivation.

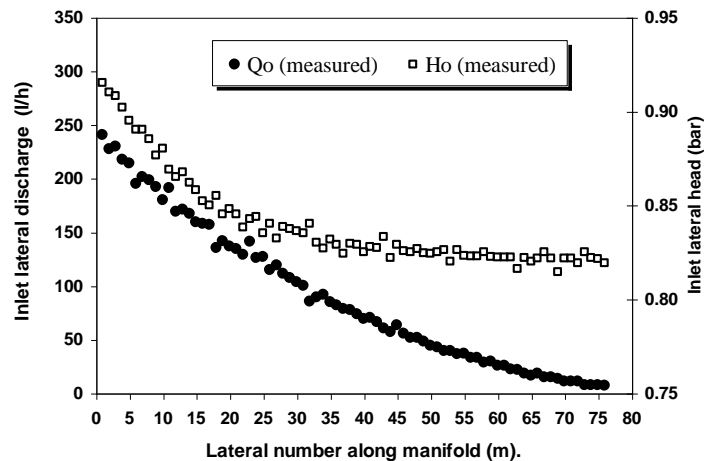


**Fig. (7) Measured inlet lateral discharge and pressure head along manifold for grape center pivot corner area, approximately triangular shape subunit, of part 1, ( $R=450$  m, with 16 mm lateral diameter).**

**Case study 1: ( $R=270$  m and  $D=16$  mm lateral diameter):**

**Part 1** which represented approximately triangular shape with angle of  $90^\circ$ , the horizontal and vertical lengths was equal to 190.9 and 79.1 m, respectively. Whereas, the minimum lateral length (LL-min) was equal to 2 m and the model found that, there is died area that has a horizontal died length was equal to 42.4 m. This area dose not contains any lateral and manifold lines.

In this case the manifold line was parallel to horizontal Cartesian with length 157.7m, while lateral lines were perpendicular on it. Maximum lateral length (LL-max) was estimated by model and was equal to 76 m. The number of emitters (E. No.) per this part was equal to 1783 emitter and number of lateral lines (L. No.) for this part was equal to 63 laterals.

Output results obtained from model clear that, average emitter discharge ( $qq_{ave}$ ) was equal to 3.68 l/h and the total discharge (QM) was equal to 6.57 ( $m^3/h$ ) with manifold diameter 50 mm. The important statistical items obtained from model such as ( $Q_{VAR}$ ), ( $H_{VAR}$ ), ( $E_u$ ) and ( $U_c$ ) for overall subunit irrigation network were found to be 4.75, 9.29, 94.2 and 89.5%, respectively. The total operating head was found to be 1.31 m.

**Part 2** which represented approximately triangular shape with angle of  $90^\circ$ , the horizontal and vertical lengths were equal to 79.1 and 190.9 m, respectively. Whereas, the minimum lateral length (LL-min) was equal to 2 m and the model found that, there is died area that has a horizontal died length was equal to 1.98 m. This area dose not contains any lateral and manifold lines.

In this case the manifold line was parallel to horizontal direction with length 77.5 m, while lateral lines were perpendicular on it. Maximum lateral

length (LL-max) was estimated by model and was equal to 157.3 m. The number of emitters (E. No.) per this part was equal to 1802 emitter and number of lateral lines (L. No.) for this part was equal to 31 laterals.

Output results obtained from model clear that, average emitter discharge ( $qq_{ave}$ ) was equal to 3.74 l/h and the total discharge (QM) was equal to 6.73 ( $m^3/h$ ) with manifold diameter 50 mm. The important statistical items obtained from model such as ( $Q_{VAR}$ ), ( $H_{VAR}$ ), ( $E_u$ ) and ( $U_c$ ) for overall subunit irrigation network were found to be 9.06, 17.3, 89.9 and 62.8%, respectively. Low ( $U_c$ ) was due to long lateral length. The total operating head was found to be 1.79 m.

**Part 3** which represented square shape with dimension 79.1x79.1 m. The model designed this area on one telescopic manifold and was parallel to horizontal Cartesian. The manifold lengths versus diameters were 67.5 and 10.0 m for 50.0 and 63 mm, respectively. The lateral lines were perpendicular on the manifold in two side directions. The lateral length was found to be approximately 40.0 m as shown in Fig (1A). The number of emitters (E. No.) in this part was equal to 2480 emitter and number of lateral lines (L. No.) for this part was equal to 62 laterals.

Output results obtained from model clear that, average emitter discharge ( $qq_{ave}$ ) was equal to 3.76 l/h and the total discharge (QM) was equal to 9.10 ( $m^3/h$ ) with manifold diameters 50 and 63 mm. The important statistical items obtained from model such as ( $Q_{VAR}$ ), ( $H_{VAR}$ ), ( $E_u$ ) and ( $U_c$ ) for overall subunit irrigation network were found to be 2.90, 5.72, 98.0 and 97.8%, respectively. The total operating head was found to be 1.19 m.

Although, approximately triangular shapes of part one and part two as shown in Fig (1A), were equal in size, there is a large difference in the values of ( $Q_{VAR}$ ) and ( $H_{VAR}$ ) ranged from (4.76 and 9.06%) to (9.29 and 17.30%), respectively. This may be due to difference in manifold and lateral lengths. Whereas, maximum lateral lengths were equal to 76 m for part one and 157.3 m for part two. This means that, friction losses at part two was grater than part one that lead to increase the value of ( $H_{VAR}$ ). The difference of dynamic head (1.31 and 1.79 bar) in both parts was due to difference in emitter discharges, that causes large discharge variations.

The telescopic manifold lengths versus diameters were varied from part to part and the other output results obtained from model were summarized in table (1)

Table 1. Output modeling for center pivot corner ( $R=270$  m, 16 mm).

Part No.	LL, (m).		E No.	L No.	$qq_{ave}$ , (l/h).	Manifold length, (m).				QM ( $m^3/h$ ).	$Q_{VAR}$ , (%)	$H_{VAR}$ , (%)	$E_u$ , (%)	$U_c$ , (%)	TH, (bar)
	Min	Max				50, mm	63, mm	75, mm	90, mm						
1	2	76	1783	63	3.684	157.5	--	--	--	6.57	4.76	9.29	94.21	89.51	1.31
2	2	157.3	1802	31	3.737	77.5	--	--	--	6.73	9.06	17.3	89.95	62.81	1.79
3	40	40.0	2480	62	3.761	67.5	10	--	--	9.1	2.9	5.72	98.03	97.76	1.19
SUM			6065			302.5	10	0	0	22.4					

refer to two-side laterals along manifold.

**Case study 2: (R=359 m and D=16 mm lateral diameter):**

In this case the model divided the whole center pivot corner area into seven parts (four parts represented approximately triangular shape with angle of 90°, two parts represented triangular shape and one square part), each part has own dimension as shown in Fig (2B). The manifold line was parallel to horizontal Cartesian, while lateral lines were perpendicular on it. The computation using model provided the values of average emitter discharge, total discharge, ( $Q_{VAR}$ ), ( $H_{VAR}$ ), ( $E_U$ ), ( $U_C$ ) and total operating head. These values were ranged from 3.65 to 3.737 l/h, 2.13 to 16.64 (m<sup>3</sup>/h), 1.32 to 6.97%, 2.62 to 12.23%, 93.03 to 98.81%, 69.46 to 97.59% and 0.94 to 1.53 m, respectively.

The telescopic manifold lengths versus diameters were varied from part to part and the other output results obtained from model were summarized in table (2)

Table 2. Output modeling for center pivot corner (R=359 m, 16 mm).

Part No.	LL, (m).		E No.	L No.	qq <sub>aver</sub> , (l/h).	Manifold length, (m).				QM, (m <sup>3</sup> /h).	Q <sub>VAR</sub> , (%).	H <sub>VAR</sub> , (%).	E <sub>U</sub> , (%).	U <sub>C</sub> , (%).	TH, (bar)
	Min	Max				50, mm	63, mm	75, mm	90, mm						
1	2	50	1169	59	3.65	147.5	---	---	---	4.27	2.31	4.57	97.4	96.19	1.04
2	2	49.05	585	25	3.636	62.5	---	---	---	2.13	1.32	2.62	98.81	97.59	0.94
3	2	61.84	588	20	3.6409	50	---	---	---	2.14	1.66	3.29	98.54	96.32	0.97
4	2	155.8	1251	21	3.704	52.5	---	---	---	4.63	6.966	13.44	93.03	69.46	1.51
5	53	53	1378	26	3.692	65	---	---	---	5.09	4.05	7.94	97.24	96.05	1.25
6	53	53.0	4450	84	3.737	50	42.5	12.5	---	16.64	6.31	12.23	95.55	95	1.53
7	67	67	1743	26	3.73	65	---	---	---	6.5	6.12	11.86	95.77	93.2	1.5
SUM			11164			492.5	42.5	12.5	0	41.4					

<sup>1</sup>refer to two-side laterals along manifold.

**Case study 3: (R=450 m and D=16 mm lateral diameter):**

In this case the model divided the whole center pivot corner area into nine parts (seven parts represented approximately triangular shape with angle of 90°, five parts represented triangular shape and one square part), each part has own dimension. The manifold line was parallel to horizontal Cartesian, while lateral lines were perpendicular on it. The computation using model provided the values of average emitter discharge, total discharge, ( $Q_{VAR}$ ), ( $H_{VAR}$ ), ( $E_U$ ), ( $U_C$ ) and total operating head. These values were ranged from 3.633 to 3.678 l/h, 1.39 to 2.26x4 (m<sup>3</sup>/h), 1.20 to 4.26%, 2.39 to 8.34%, 94.92 to 99.03%, 92.01 to 98.68% and 0.92 to 1.26 m, respectively.

The telescopic manifold lengths versus diameters were varied from part to part and the other output results obtained from model were summarized in table (3).

In this case the model divided the whole center pivot corner area into nineteen

parts (ten parts represented approximately triangular shape with angle of 90°, eight parts represented triangular shape and one square part) as shown in Fig. (8B), each part has own dimension. The manifold line was parallel to horizontal Cartesian, while lateral lines were perpendicular on it. The computation using model provided the values of average emitter discharge, total discharge, ( $Q_{VAR}$ ), ( $H_{VAR}$ ), ( $E_U$ ), ( $U_C$ ) and total operating head. These

values were ranged from 3.627 to 3.780 l/h, 1.60 to 32.43x4 (m<sup>3</sup>/h), 0.72 to 16.12%, 1.44 to 16.08%, 93.90 to 99.88%, 84.29 to 98.46% and 0.88 to 1.81 m, respectively.

**Table 3. Output modeling for center pivot corner (R=450 m, 16 mm).**

Part No.	LL, (m).		E No.	L No.	qq <sub>ave</sub> , (l/h).	Manifold length, (m).				QM (m <sup>3</sup> /h).	Q <sub>VAR</sub> , (%).	H <sub>VAR</sub> , (%).	E <sub>U</sub> , (%).	U <sub>C</sub> , (%).	TH, (bar)
	Min	Max				50, mm	63, mm	75, mm	90, mm						
1	2	63.1	1863	76	3.678	190	---	---	---	6.85	4.26	8.34	94.92	92.58	1.26
2	2	62.9	954	32	3.653	80	---	---	---	3.49	2.51	4.93	97.62	95.23	1.06
3	2	81.4	994	26	3.663	65	---	---	---	3.64	3.3	6.5	96.89	92.01	1.14
4	2	61.2	383	13	3.633	32.5	---	---	---	1.39	1.2	2.39	99.03	96.97	0.92
5	2	126.6	675	13	3.663	32.5	---	---	---	2.47	3.78	7.41	96.73	84.12	1.15
6	33	33.0 <sup>*</sup>	2178	66	3.658	82.5	---	---	---	7.97	2.19	4.33	98.52	98.52	1.04
7	33	33.0 <sup>*</sup>	1716 x4	52x4	3.649	65x4	---	---	---	6.26x4	1.75	3.47	98.83	98.68	0.99
8	42	42.0 <sup>*</sup>	2184	52	3.666	62.5	2.5	---	---	8.01	2.69	5.3	98.19	97.7	1.09
9	66	66	858	13	3.675	32.5	---	---	---	3.15	3.12	6.33	97.93	95.35	1.14
SUM			16953			545	2.5	0	0	33.82					

<sup>\*</sup>refer to two-side laterals along manifold.

2 or 4 refer to number of subunit division inside part (N).

#### **Case study 4: (R=450 m and D=16 mm lateral diameter):**

The telescopic manifold lengths versus diameters were varied from part to part and the other output results obtained from model were summarized in table (4)

**Table 4. Output modeling for center pivot corner (R=450 m, 16 mm).**

Part No.	LL, (m).		E No.	L No.	qq <sub>ave</sub> , (l/h).	Manifold length, (m).				QM (m <sup>3</sup> /h).	Q <sub>VAR</sub> , (%).	H <sub>VAR</sub> , (%).	E <sub>U</sub> , (%).	U <sub>C</sub> , (%).	TH, (bar)
	Min	Max				50, mm	63, mm	75, mm	90, mm						
1	1	32.5	3533	139	3.687	114	25	---	---	13.03	4.73	9.24	94.15	93.6	1.33
2	1	32.4	1946	63	3.66	63	---	---	---	7.12	2.88	5.67	97.09	95.78	1.11
3	1	29.5	1215	42	3.643	42	---	---	---	4.43	1.76	3.49	98.32	97.16	0.99
4	1	32.4	1147	36	3.64	36	---	---	---	4.18	1.82	3.61	98.28	96.75	0.99
5	1	35.6	1120	32	3.645	32	---	---	---	4.08	1.95	3.86	98.18	96.14	1
6	1	40	1096	28	3.647	28	---	---	---	4	2.13	4.22	98.03	95.29	1.02
7	1	27.7	442	16	3.627	16	---	---	---	1.6	0.72	1.44	99.4	98.44	0.88
8	1	44.6	686	16	3.639	16	---	---	---	2.5	1.64	3.25	98.6	95.25	0.96
9	1	44.6	686	16	3.639	16	---	---	---	2.5	1.64	3.25	98.6	95.25	0.96
10	1	76.2	986	15	3.662	15	---	---	---	3.61	3.65	7.17	96.76	84.29	1.15
11	33	33	4290	65	3.78	32	27	6	---	16.22	8.39	16.08	93.9	93.85	1.81
12	33	33.0 <sup>*</sup>	10824	164	3.72	32	28	22	---	40.26	5.47	10.64	96.14	95.1	1.43
13	33	33	2706	41	3.72	32	9	---	---	10.07	5.47	10.64	96.14	95.1	1.43
14	33	33	8580x4	130x4	3.78	16x4	14x4	12x4	23x4	32.43x4	8.39	16.08	93.9	93.85	1.81
15	36	36	2376	33	3.714	29	4	---	---	8.83	5.21	10.15	96.36	94.62	1.39
16	41	41	5412x2	66'2	3.741	13x2	11x2	9x2	---	20.24x2	6.54	12.66	95.39	92.73	1.56
17	28	28	896	16	3.648	16	---	---	---	3.27	1.72	3.41	98.88	97.91	0.99
18	33	33.0 <sup>*</sup>	4356	66	3.701	16	14	3	---	16.12	4.47	8.75	96.89	95.6	1.3
19	48	48	1536	16	3.699	16	---	---	---	5.68	4.5	8.8	97.01	92.68	1.29
SUM			84985			641	185	97	92	317.7					

<sup>\*</sup>refer to two-side laterals along manifold.

2 or 4 refer to number of subunit division inside part (N).

**Case study 5: (R=450 m and D=18 mm lateral diameter):**

In this case the model divided the whole center pivot corner area into thirteen parts (seven parts represented approximately triangular shape with angle of 90°, five parts represented triangular shape and one square part) as shown in Fig. (8A), each part has own dimension. The manifold line was parallel to horizontal Cartesian, while lateral lines were perpendicular on it. The computation using model provided the values of average emitter discharge, total discharge, ( $Q_{VAR}$ ), ( $H_{VAR}$ ), ( $E_U$ ), ( $U_C$ ) and total operating head. These values were ranged from 3.627 to 3.740 l/h, 2.49 to 31.63x4 (m<sup>3</sup>/h), 0.71 to 6.51%, 1.41 to 12.59%, 94.28 to 99.40%, 89.50 to 97.95% and 0.94 to 1.56 m, respectively.

The telescopic manifold lengths versus diameters were varied from part to part and the other output results obtained from model were summarized in table (5)

**Case study 6: (R=450 m and D=20 mm lateral diameter):**

In this case the model divided the whole center pivot corner area into thirteen parts (seven parts represented approximately triangular shape with angle of 90°, five parts represented triangular shape and one square part) as shown in Fig. (8A), each part has own dimension.

Table 5. Output modeling for center pivot corner (R=450 m, 18 mm).

Part No.	LL, (m).		E No.	L No.	qq <sub>ave</sub> , (l/h).	Manifold length, (m).				QM (m <sup>3</sup> /h).	Q <sub>VAR</sub> , (%)	H <sub>VAR</sub> , (%)	E <sub>U</sub> , (%)	U <sub>C</sub> , (%)	TH, (bar)	
	Min	Max				50, mm	63, mm	75, mm	90, mm							
1	1	32.5	3533	139	3.648	115	24	---	---	12.89	2.07	4.1	97.47	97.24	1.03	
2	1	32.4	1946	63	3.636	63	---	---	---	7.08	1.25	2.49	98.74	98.18	0.94	
3	1	65.4	5068	82	3.697	55	19	9	---	18.74	5.29	10.3	94.28	89.5	1.4	
4	1	76	4592	65	3.681	49	16	---	---	16.9	4.3	8.41	95.48	90.79	1.28	
5	1	64.6	2016	33	3.651	33	---	---	---	7.36	2.41	4.77	97.65	93.25	1.05	
6	1	44.6	686	16	3.627	16	---	---	---	2.49	0.71	1.41	99.4	97.95	0.87	
7	1	76.2	986	16	3.642	16	---	---	---	3.59	2.06	4.07	98.15	90.48	1	
8	33	33	4291	65	3.686	33	28	4	---	15.82	3.72	7.3	97.36	97.34	1.22	
9	33	33.0	10824	166	3.706	16	14	13	39	40.11	4.69	9.17	96.63	96.99	1.34	
10	33	33.0	8580x4	130x4	3.687	16x4	14x4	13x4	22x4	31.63x4	3.72	7.3	97.36	97.34	1.22	
11	41	41	10824	130	3.725	13	11	10	31	40.32	5.68	11.05	95.91	95.35	1.46	
12	66	66	4356	33	3.74	16	14	3	---	16.03	6.51	12.59	95.39	90.84	1.56	
13	48	48	1536	16	3.653	16	---	---	---	5.61	1.97	3.9	98.71	96.84	1.01	
SUM			84978			505	182	91	158	313.46						

refer to two-side laterals along manifold.

2 or 4 refer to number of subunit division inside part (N).

The manifold line was parallel to horizontal Cartesian, while lateral lines were perpendicular on it. The computation using model provided the values of average emitter discharge, total discharge, ( $Q_{VAR}$ ), ( $H_{VAR}$ ), ( $E_U$ ), ( $U_C$ ) and total operating head. These values were ranged from 3.627 to 3.740 l/h, 2.49 to 31.63x4 (m<sup>3</sup>/h), 0.47 to 4.35%, 0.94 to 8.52%, 96.22 to 99.17%, 93.07 to 99.79% and 0.85 to 1.29 m, respectively.

The telescopic manifold lengths versus diameters were varied from part to part and the other output results obtained from model were summarized in table (6).

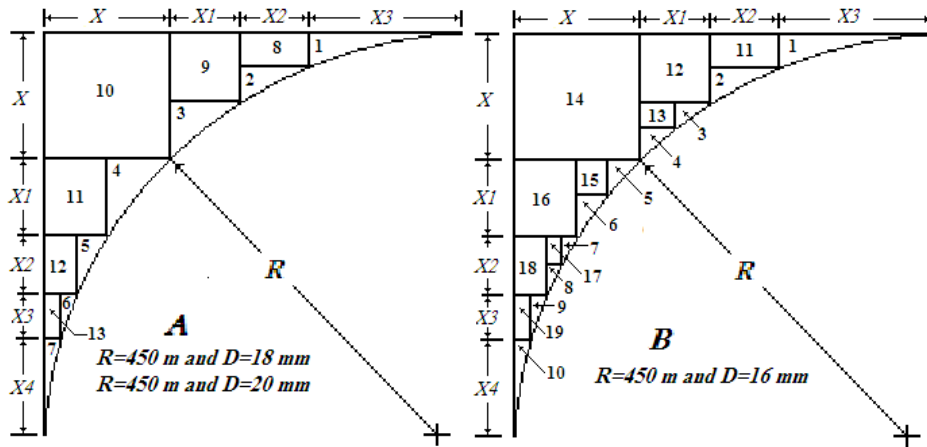


**Fig. (8) Modeling design steps for dividing whole area of center pivot corner under different lateral diameters (16, 18 and 20 mm) for center pivot radius 450 m.**

Table 6. Output modeling for center pivot corner ( $R=450$  m, 20 mm).

Part No.	LL, (m).		E No.	L No.	qq <sub>ave</sub> , (l/h).	Manifold length, (m).				QM (m <sup>3</sup> /h).	Q <sub>VAR</sub> , (%)	H <sub>VAR</sub> , (%)	E <sub>U</sub> , (%)	U <sub>C</sub> , (%)	TH, (bar)	
	Min	Max				50, mm	63, mm	75, mm	90, mm							
1	1	32.5	3533	139	3.637	115	24	---	---	12.89	1.37	2.73	98.32	98.17	0.95	
2	1	32.4	1946	63	3.636	63	---	---	---	7.08	0.83	1.65	99.17	98.79	0.89	
3	1	65.4	5068	82	3.697	55	19	9	---	18.74	3.53	6.94	96.22	93.07	1.19	
4	1	76	4592	65	3.681	49	16	---	---	16.9	2.86	5.64	97.02	93.92	1.11	
5	1	64.6	2016	33	3.651	33	---	---	---	7.36	1.6	3.18	98.45	95.54	0.97	
6	1	44.6	686	16	3.627	16	---	---	---	2.49	0.47	0.94	99.6	98.65	0.85	
7	1	76.2	986	16	3.642	16	---	---	---	3.59	1.36	2.71	98.78	93.71	0.93	
8	33	33	4291	65	3.686	33	28	4	---	15.82	2.47	4.89	98.25	98.24	1.08	
9	33	33.0	10824	166	3.706	16	15	12	39	40.11	3.13	6.16	97.77	98.01	1.15	
10	33	33.0	8580x4	130x4	3.687	16x4	15x4	12x4	22x4	31.63x4	2.47	4.89	98.25	98.24	1.08	
11	41	41	10824	130	3.725	13	11	10	31	40.32	3.8	7.45	97.29	96.92	1.23	
12	66	66	4356	33	3.74	16	15	2	---	16.03	4.35	8.52	96.95	93.94	1.29	
13	48	48	1536	16	3.653	16	16	---	---	5.61	1.31	2.59	99.15	97.91	0.94	
SUM			84978			505	204	85	158	313.46						

refer to two-side laterals along manifold.

2 or 4 refer to number of subunit division inside part (N).

The computation using model provided information about number of emitters in each design part for all cases studies. These computations were summarized in table (1).to table (6). Emitters number predicted for case study No. one, two and three for center pivot radius 270, 359 and 450 m (lateral spacing 2.5 m and emitter spacing 1.0 m) for grape cultivation, were 6065, 11164 and 16953, respectively using lateral diameter 16 mm. These variations were corresponding to number of parts which divided to small areas by model to reduce (Q<sub>VAR</sub>), (H<sub>VAR</sub>). Most pipe lines required in modeling design, the telescopic manifold length and diameter was found for 50 mm. While, manifold diameter 90 mm dose not appear,

On the other hand, emitters number predicted for case study No. four, five and six for center pivot radius 450 m using lateral diameter 16, 18 and 20 mm (lateral spacing 1.0 m and emitter spacing 0.5 m) for strawberry

cultivation were 84985, 84978 and 84978, respectively,. Slightly variations were found in emitter's number between case study four and five or six, which represented to constant parts area (13 parts). Most pipe lines required in modeling design, the telescopic manifold lengths and diameters were found for 50 mm. Also, pipe line requirement for manifold diameter 90 mm were ranged from 92 to 157 m.

In comparison between model results output of center pivot corner with R=450 m for lateral diameters (18 and 20 mm), it is clear that the number of parts dose not changed (13 parts) and total manifold discharge was equal to 313.46 ( $m^3/h$ ) for both lateral diameters. There is a slightly variations in manifold length for diameter 63 and 75 mm, were 182 and 91 m for lateral diameter 18 mm, while 204 and 85 m for lateral diameter 20 mm. However, lateral diameter 20 mm was more effect in improving ( $Q_{VAR}$ ) and ( $H_{VAR}$ ). The values of ( $Q_{VAR}$ ) for 13 parts at lateral diameter 18 and 20 mm were ranged from (0.7 to 6.51%) and (0.47 to 4.35%) respectively. Also, ( $H_{VAR}$ ) for the same condition were ranged from (1.14 to 12.59%) and (0.94 to 8.52%) respectively.

There is remarkable difference in manifold lengths versus diameters and total manifold discharge in case study R=450 m with lateral diameter (16 mm). The model divided the whole area of center pivot corner into (19 parts). Manifold lengths were equal to 641, 185, 97, and 92 m for 50, 63, 75, and 90 mm, respectively, as compared with lateral diameter (18 mm), manifold lengths were 505, 182, 91 and 158 m for the same manifold diameters. While, with lateral diameter (20 mm), manifold lengths were 505, 204, 85, and 158 m for the same manifold diameters.

## **CONCLUSIONS**

The simulation model of center pivot corners that uses fundamental hydraulic relationships to simulate flow within micro-irrigation network was developed. The model takes into account the change in water viscosity due to temperature. The model operates well and is capable of predicting with successive accurately any emitter discharge ( $qqi$ ) along any lateral, each emitter operating head and discharge for all laterals and average emitter discharge per lateral. The model was tested and validated for hydraulic lateral with different lengths and segment manifold design (discharge, operating head, diameter, discharge and operating head variation, emission uniformity and uniformity coefficient) for each part of design under different center pivot radiiuses and different lateral diameters. The measured values obtained from the experimental field are closely agreement with the predicted values obtained from model. The proposed methodology is computationally efficient and can help irrigation consultants in the design of micro-irrigation system. In arid and semiarid regions, design is important to increase yields and to conserve water and soil as well as the economical utilization of power.

## **REFERENCES**

- Amer, K. H and A. H. Gomaa (2003). Uniformity determination in micro-irrigation lateral design. Misr J. Ag. Eng., 20 (2): 405-434.
- Al-Amoud, A.I. (1997). Analysis of pressure drop due to emitter in micro-irrigation lateral connections. Agric. Univ. Cairo Bulletin, 47: 213-234.
- Al-Misned, A., A. Al-Amoud and H. Hathoot (2000). Effect of energy loss due to emitters on the design of micro-irrigation laterals. J. King Saud Univ., Vol. 12, Agric. Sci. (2): 107-120.
- Antonina, C. and B. Scicolone (1998). Water quality and distribution uniformity drip/micro-irrigation systems. J. Agric. Eng. Res., 70: 355-365.
- ASAE (2002a), Design and installation of micro-irrigation systems. ASAE, St. Joseph, Mich., USA. ASAE STANDARDS, EP405. 1 DECO1.
- ASAE (1996). ASAE standards engineering practices data. 43rd edition. MI, USA.: 864.
- EL-Nesr, M. N. (1999). Computer aided design and planning of micro-irrigation systems. M.Sc. Agric. Eng., Faculty of Agriculture, Alexandria University.
- Hathoot, H.M., A.I. Al-Amoud and F.S. Mohammed (1993). Analysis and design of micro-irrigation laterals. J. Irrig. Drain. Div., ASCE, 119 (5): 756-767.
- Guirguis A. E; A. El-Shafei and Kh. A. Allam (2009). Mathematical model for subunit drip irrigation system design. J. Agric. Sic. Mansoura Univ., 34 (4): 4011-4029.
- Ismail, S. M. (1993). Hydraulic simulation of micro-irrigation system. Alex. J. Agric. Res., 38 (3): 25-43.
- Ismail, S. M; E.R. El-Ashry; G.A.Sharaf; and M. N.El-Nesr (2001). Computer aided design of trickle irrigation system. Misr. J. Agric. Eng. 18 (2): 243-2600.
- Keller, J. and D. Karmeli (1974). Micro-irrigation design parameters. Trans. of the ASAE: 678-684.
- Sharaf, D. A. (2004a). A study of water distribution uniformity of micro irrigation subunit. Misr. J. Agric. Eng. 21 (1): 103-124.
- Sharaf, D. A. (2004b). Improving micro irrigation efficiency by pressure regulated emission devices. Misr. J. Agric. Eng. 21 (1): 139-153.
- Smith, A. (2003). Water management and the land management planning process: A User Aid. National Center for Engineering in Agriculture Publication. 1000022/3, USA.
- Zella, L and A. Kettab (2002). Numerical methods of microirrigation lateral design. Biotechnol. Agron. Soc. Environ. 2002 6 (4), 231–235.
- Zella, L, A. Kettab and Ch. Gérard. (2006) Design of a micro-irrigation system based on the control volume method. Biotechnol. Agron. Soc. Environ. 10 (3), 163 – 171.

## نموذج رياضي لتصميم الري بالتنقيط لأركان الري بالرش المحوري آمون القمص جرجس<sup>١</sup> - احمد عبد الله الشافعى<sup>٢</sup> وخليل عبد الحليم علام<sup>٣</sup> <sup>١</sup>معهد بحوث الهندسة الزراعية، مركز البحوث الزراعية، الدقى، جيزه، ج.م.ع. <sup>٢</sup>قسم الهندسة الزراعية كلية الزراعة جامعة الإسكندرية.

نظام الري بالرش المحوري شائع الاستخدام في جميع أنحاء العالم ولاسيما في المناطق ذات المناخ الحار والشبيه حار. ونظراً للمساحة الدائرية التي يغطيها الري بالرش المحوري فإنه توجد مساحات بالأركان لا يمكن تغطيتها بهذا النظام. ولتحقيق الأستفادة من التوسيع الأفقي للمساحات التي يتم ريها بنظام الري بالرش المحوري، فقد قام العديد من المستثمرون برب الأركان بنظام الري بالتنقيط والتي تمثل مساحة ٢١,٥٪. ونظراً لأنخفاض كفاءة الري بالتنقيط بالأركان وذلك لقلة خبرة وقلة المعلومات للقائمين على التنفيذ، ونظراً لندرة الأبحاث التي قامت بدراسة الري بالتنقيط بالأركان وقلة خبرة المنفذون وعدم الوضع في الاعتبار المعايير التصميمية ولاسيما انتظامية توزيع المياه ( $E_{UC}$ ) - معامل توزيع المياه ( $U_C$ ) - نسبة التغير في التصرف ( $QVAR$ ) (ونسبة التغير في الضغط ( $HVAR$ ) لذا كان الهدف من البحث هو وضع بعض المحاولات التصميمية لتنفيذ شبكة رى بالتنقيط للأركان مع الأخذ في الاعتبار المعايير التصميمية التي ترفع من كفاءة الشبكة ولاسيما أن لا تقل نسبة التغير في التصرف عن ١٠٪ ونسبة التغير في الضغط عن ٢٠٪.

لذا كانت أهداف البحث هي:  
 ١- تطوير نموذج رياضي بالكمبيوتر لتقسيم وتصميم القطع الفرعية للري بالتنقيط لرى الأركان (micro-irrigation network) مشتملاً على التصميم الهيدروليكي لكل من خطوط النقاط (Lateral lines) والمشعبات (Manifold lines) وتقدير قيم كل من انتظامية توزيع المياه ( $E_{UC}$ ) - معامل توزيع المياه ( $U_C$ ) - نسبة التغير في التصرف ( $QVAR$ ) - نسبة التغير في الضغط ( $HVAR$ ).  
 ٢- اختبار صحة نتائج النموذج الرياضي والتأكيد من مصداقية وذلك بمقارنته بنتائج التجارب الحقلية.  
 ٣- اختبار حساسية النموذج الرياضي في تصميم الأركان لنظام الري بالرش المحوري مختلف الأقطار والمتابعة التجارب.  
 تم عمل نموذج رياضي وبعد أجزاء التجارب الاختبارية عليه والتأكد من صحته ومصداقته ودقته، تم أجراء بعض التجارب الحقلية بشركة الأسكتدرية الزراعية-غرب النوبالية-محافظة البحيرة على نظام رى بالرش المحوري (Center pivot corner) بقطر ٤٥٠ م وخطوط تنقيط بقطار ٦١ م خلال موسم ٢٠٠٨ وقد قام النموذج الرياضي بتقسيم الركن إلى عدد من الأجزاء لتخفيف قيمة كل من ( $QVAR$ ) و( $HVAR$ ) بحيث لا تزيد قيمتهما عن المسموح به وهو ١٠٪ و ٢٠٪ على الترتيب وتم اخذ القياسات المقابلة ومقارنتها بنتائج المتحصل عليها. وكانت أهم النتائج المتحصل عليها من البحث هي:

تم اختبار صحة النموذج الرياضي لنتائج لجزء شبة المثلث رقم ١ لكل من متوسط تصرف النقاطات لكل خط من خطوط النقاطات (٧٦) نسبة التغير في التصرف ( $QVAR$ ) و نسبة التغير في ( $HVAR$ ) وأنظمة توزيع المياه ( $E_{UC}$ ) . و معامل توزيع المياه ( $U_C$ ) كما يلى:

١. متوسط تصرف النقاطات لكل خط تنقيط من خطوط النقاطات (٧٦) كانت يتراوح بين ٣,٦١٨ إلى ٣,٧٦٦ لتر/س. حدوث انخفاض في متوسط تصرف النقاطات لكل خط تنقيط بزيادة طول الخط المشعب. هذا الانخفاض بسبب الفاقد في الاحتكاك وكان متوسط نسبة الانحراف ١٨٪. هذا يعني أن النموذج الرياضي قادر على التنبؤ بالتصريف المتوسط للنقاطات لكل خط من خطوط النقاطات وبدقة عالية.

٢. القيم المتباينة بها والمحسوبة من نتائج التجارب الحقلية ( $QVAR$ ) و ( $HVAR$ ) لكل خط تنقيط من خطوط النقاطات (٧٦) على طول الخط المشعب كانت قريبة جداً وكان متوسط نسبة الانحراف لهما ١,٩٣٪ و كانت قيمة ( $R^2$ ) تساوي ٠,٩٥٪ و ٠,٩٥٪ على الترتيب.

٣. قيمة ( $E_{UC}$ ) وقيمة ( $U_C$ ) لخطوط النقاطات (٧٦) كانت تتراوح بين ٩٤,٩٪ إلى ٩٩,٣٪ و ١٢٪ إلى ٨٤,١٪ على الترتيب. وكانت القيمة المتوسطة لنسبة الانحراف لها هي ٢,١٦٪ و ٢,٢٢٪ وكانت قيمة ( $R^2$ ) لهما تساوى ٠,٩٦٥٪ و ٠,٩٧٦٪ على الترتيب. هذا يعني أن النموذج الرياضي قادر على التنبؤ بمتوسط قيمة ( $E_{UC}$ ) وقيمة ( $U_C$ ) بصورة جيدة وسريعة وكانت القيم المتناوبة لها تتفوق ٩٤,٩٪.

٤. زيادة الضاغط الديناميكي لخطوط النقاطات (٧٦) على طول الخط المشعب من ٠,٨١ إلى ١,٢٦ بار وقيمة ( $U_C$ ) زادت بنسبة ٧,٤٪. هذا يعني أن قيمة ( $U_C$ ) تزداد مع انخفاض الفاقد في الاحتكاك لخطوط النقاطات.

٥. التصرف الماء خلال أجزاء الخط المشعب لخطوط النقاطات (٧٦) كانت يتراوح بين ٢٤,٠٪ إلى ٦,٨٥٪. لكل من أصغر خط تنقيط (٢ متر) والمجاور (deid area) وأكبر خط تنقيط (٦٣ متر) على الترتيب. هذا يعني أن قيمة التصرف خلال أجزاء الخط المشعب تعتمد على عدد النقاطات بكل خط

#### تنقيط وعدد خطوط التقطيف.

٦ كانت قيم أطوال الخط المشعب لخطوط النقاطات (٧٦) تساوي ١٩٠ متر وبقطر ٥٠ مم بينما للجزء رقم ٨ كانت قيم أطوال الخط المشعب ٦٢,٥ و ٢,٥٥ متر للاقطار ٥٠ و ٦٣ مم على الترتيب. تغير قطر الخط المشعب يعتمد على التصرف الكلي المار به (عدد خطوط التقطيف وما تحملة من عدد النقاطات). من النتائج يتضح أن النموذج الرياضي نجح بصورة جيدة في التنبؤ بطول الخط المشعب وأقطاره.

تم اختبار حساسية النموذج الرياضي لثلاث حالات تمثل أنصاف الأقطار المختلفة للري بالرش المحوي (٢٧٠ و ٣٥٩ و ٤٥٠ متر) مع قطر لخطوط التقطيف (١٦ مم) والمسافة بين النقاطات (١ متر) والمسافة بين خطوط التقطيف (٢,٥ متر) ل النوع واحد من النقاطات ( $q=4.02H^{0.5}$ ) وهذه الحالة تمثل زراعة العنب. وتلذ حالات أخرى تمثل نصف قطر ثابت للري بالرش المحوي (٤٥٠ متر) مع أقطار لخطوط التقطيف (١٦ و ١٨ و ٢٠ مم) والمسافة بين النقاطات (٥,٥ متر) والمسافة بين خطوط التقطيف (١ متر) ولنفس نوع النقاط وهذه الحالة تمثل زراعة الفراولة.

١ عدد النقاطات المتبناً بها لأنصاف الأقطار المختلفة للري بالرش المحوي (٢٧٠ و ٣٥٩ و ٤٥٠ متر) مع قطر لخطوط التقطيف (١٦ مم) كانت ٦٠٦٥ و ١١١٦٥ و ١٦٩٥٣ على الترتيب. معظم أطوال خطوط المشعبات المتبناً بها كانت للقطر (٥٠ مم) ولم يظهر القطر (٩٠ مم) والاختلاف في عدد النقاطات يرجع إلى الاختلاف في مساحة الاركان وعدد خطوط التقطيف وما تحملة من نقاطات. أما عدد النقاطات المتبناً بها للري بالرش المحوي (٤٥٠ متر) مع قطر لخطوط التقطيف (١٦ و ١٨ و ٢٠ مم) كانت ٨٤٩٨٥ و ٨٤٩٧٨ و ٨٤٩٧٨ على الترتيب. معظم أطوال خطوط المشعبات المتبناً بها كانت للقطر (٥٠ مم) والقطر (٩٠ مم) كان يتراوح بين ٩٢ و ١٥٨ متر.

٢ مقارنة القيم المتبناً بها عند استخدام نصف قطر للري بالرش المحوي (٤٥٠ متر) مع أقطار خطوط التقطيف (١٨ و ٢٠ مم) أوضحت أن عدد الأجزاء التي قسمت بواسطة النموذج الرياضي لم تتغير وكانت (١٣) جزءاً. وكان التصرف المار بالمشعب (٣١٣,٤٦ م٣/س). ووُجدت اختلافات ضئيلة في أطوال المشعبات مع أقطارها (٦٣ و ٧٥ مم) وكانت ١٨٢ و ٩١ متر لخط التقطيف (١٨) (م) وكانت ٢٠٤ و ٨٥ متر لخط التقطيف (٢٠) (م).

٣ تحسنت قيمة ( $Q_{VAR}$ ) لركن الري بالرش المحوي بنصف قطر (٤٥٠ متر) مع قطر لخطوط التقطيف (١٨ و ٢٠ مم). وكانت تتراوح بين (٧,٠% الي ٧,٥%) (٤٧,٠% الي ٤٣,٥%) على الترتيب. أيضاً تحسنت قيمة ( $H_{VAR}$ ) وكانت تتراوح بين (١٤,١% الي ١٢,٥%) (٩٤,٠% الي ٨٥,٠%).

٤ القيم المتبناً بها عند استخدام نصف قطر للري بالرش المحوي (٤٥٠ متر) مع أقطار خطوط التقطيف (١٦) (م) أوضحت أن عدد الأجزاء التي قسمت بواسطة النموذج الرياضي كانت (١٩) جزءاً. وكانت أطوال خط المشعب (٦٤١ و ١٨٥ و ٩٧ و ٩٢ متر مع أقطارها (٥٠ و ٦٣ و ٧٥ و ٩٠ مم على الترتيب بالمقارنة بخطوط التقطيف (١٨) (م) كانت أطوال خط المشعب (٥٠٥ و ١٨٢ و ٩١ و ١٥٨) متر مع نفس الأقطار. أما خطوط التقطيف (٢٠) (م) فكانت أطوال خط المشعب (٥٠٥ و ٢٠٤ و ٨٥ و ١٥٨) متر مع نفس الأقطار.

٥ أوضحت النتائج أن النموذج الرياضي قادر على التنبؤ بصورة جيدة وبدقة عالية في إجراء التصميم الهيدروليكي لكل من خطوط النقاطات مختلفة الأطوال والخط المشعب للري بالتنقيط لأركان الري بالرش المحوري كما أنه قابل للتطبيق عملياً في التصميم ويساهم في العمل الاستشاري لحفظ المياه والستخدام الاقتصادي للطاقة.